# Appendix G
# Procedures and Examples for Rapid Drawdown

## G-1. General

Embankments may become saturated by seepage during a prolonged high reservoir stage. If subsequently the reservoir pool is drawn down faster than the pore water can escape, excess pore water pressures and reduced stability will result. For analysis purposes it is assumed that drawdown is very fast, and no drainage occurs in materials with low permeability. Two separate procedures for computing slope stability for rapid drawdown are presented in this appendix.

*a.* The first method is the one described in the 1970 version of this manual. It will be referred to here as the "Corps of Engineers' 1970 procedure."

*b.* The second method is the one developed by Lowe and Karafiath (1960),[1] and modified by Wright and Duncan (1987), and by Duncan, Wright, and Wong (1990). The objectives of the modifications were (1) to simplify the method, and (2) to account more accurately for shear strength in zones where drained strength is lower than undrained strength. The second method is more rational than the first, and is recommended. The first method may be unrealistically conservative for soils that dilate during shear, and may lead to uneconomical designs.

## G-2. U.S. Army Corps of Engineers' 1970 Procedure - Background

This method was presented in the previous (1970) version of this manual (USACE 1970). It involves two complete sets of stability calculations for each trial shear surface. The first set of calculations is performed for the conditions before drawdown, and is used to estimate the effective stresses to which the soil is consolidated before drawdown. Although a factor of safety is computed in the first set of calculations, the purpose of the first set of calculations is to compute the consolidation stresses. The effective stresses before drawdown are used to estimate the undrained shear strengths that would exist during rapid drawdown. These shear strengths are then used to perform a second set of stability calculations for conditions immediately after drawdown. The factor of safety from the second set of calculations is the factor of safety for the rapid drawdown condition.

*a. First-stage computations*. The first-stage computations are performed to calculate the effective stresses to which the soil is consolidated prior to drawdown. The soil strengths and pore water pressures used in the analysis are the same as those used for the long-term analysis of the steady seepage condition. Effective stress shear strength parameters derived from Consolidated-Undrained (CU or R) tests with pore water pressure measurements, or from Consolidated-Drained (CD or S) tests should be used. Pore water pressures are computed from hydrostatic conditions or an appropriate seepage analysis. External water pressures from the reservoir or other adjacent water are applied as loads to the face of the slope. The objective of the computations is to evaluate the effective stresses on the base of each slice along the assumed slip surface. The effective stresses are obtained by dividing the total normal force (N) on the base of each slice by the length of the base, and subtracting the pore water pressure, i.e.,

$$\sigma'_c = \frac{N}{\Delta\ell} - u \qquad \text{(G-1)}$$

[1] Reference information is presented in Appendix A.

The stress $\sigma'_c$ is the effective normal stress, or consolidation stress, on the slip surface before drawdown.

*b. Second-stage shear strengths*. Once the effective consolidation stresses have been calculated from the first-stage computations, shear strengths are estimated for the second stage. The shear strengths are estimated from a "composite," bilinear shear strength envelope. The envelope represents the lower bound of the R and S strength envelopes.

(1) The R envelope is determined by plotting a circle using the effective minor principal stress during consolidation, $\sigma'_{3c}$, and the principal stress difference at failure, $(\sigma_1 - \sigma_3)_f$, as shown in Figure G-1, together with the corresponding R envelope. Figure G-1a shows the envelope using conventional axes $(\sigma - \tau)$; while Figure G-1b shows the envelope on a modified diagram of $(\sigma_1 - \sigma_3)_f$ versus $\sigma_3$. Neither envelope is a valid Mohr-Coulomb envelope, because they are plotted using one stress that existed during consolidation, $\sigma'_{3c}$, and another stress that existed at failure, $(\sigma_1 - \sigma_3)_f$. Accordingly, this envelope is not consistent with the fundamental principles of soil mechanics. It is empirical and should only be used in empirical procedures like the 1970 procedure for rapid drawdown.

(2) The composite envelope used to determine the shear strengths for the second-stage computations is shown in Figure G-2. The envelope represents the lower bound of the empirical R envelope described above, and the effective stress S envelope. Shear strengths are determined for the second-stage computations using the effective normal stress calculated for the first stage (from Equation G-1) and the composite envelope shown in Figure G-2. Shear strengths are determined in this manner for each slice whose base lies in material that does not drain freely.

*c. Second-stage computations*. The second-stage computations are performed to calculate the stability immediately after drawdown. For materials that do not drain freely the shear strengths are determined in the manner described in G-2b. These strengths are assigned as values of cohesion, c, with $\phi$ equal to zero. For materials that drain freely, effective stress shear strength parameters, $c'$ and $\phi'$, are used, and appropriate pore water pressures are prescribed. The pore water pressures for free-draining materials should represent the values after drawdown has occurred and steady-state seepage has been established at the new lower water level. The pore water pressures for materials which do not drain freely are set equal to zero. If a portion of the slope remains submerged after drawdown, the external water pressures acting on the submerged part of the slope are calculated and applied as external loads to the surface of the slope.

## G-3. Improved Method for Rapid Drawdown – Background

This method was developed by Lowe and Karafiath (1960), and modified by Wright and Duncan (1987) and Duncan, Wright, and Wong (1990). The method involves either two or three separate slope stability calculations for each trial slip surface. The first computation is the same as that for the Corps of Engineers' 1970 procedure and is used to calculate the effective stresses to which the soil is consolidated before drawdown. The second set of computations is performed using undrained shear strengths corresponding to the effective consolidation stresses calculated in the first stage. If the drained shear strength is less than the undrained shear strength for any slices, a third set of calculations is performed, using drained shear strengths for those slices. The factor of safety from the last stage (the second or third stage) is the factor of safety after rapid drawdown.

*a. First-stage computations*. The first-stage computations are the same as those for the Corps of Engineers' 1970 method. However, in addition to computing the consolidation normal stress on the base of each slice, $\sigma'_c$, the shear stress at consolidation, $\tau_c$, is also calculated for each slice. The shear stress at consolidation is calculated by dividing the shear force (S) on the base of the slice by the length of the base, i.e.,

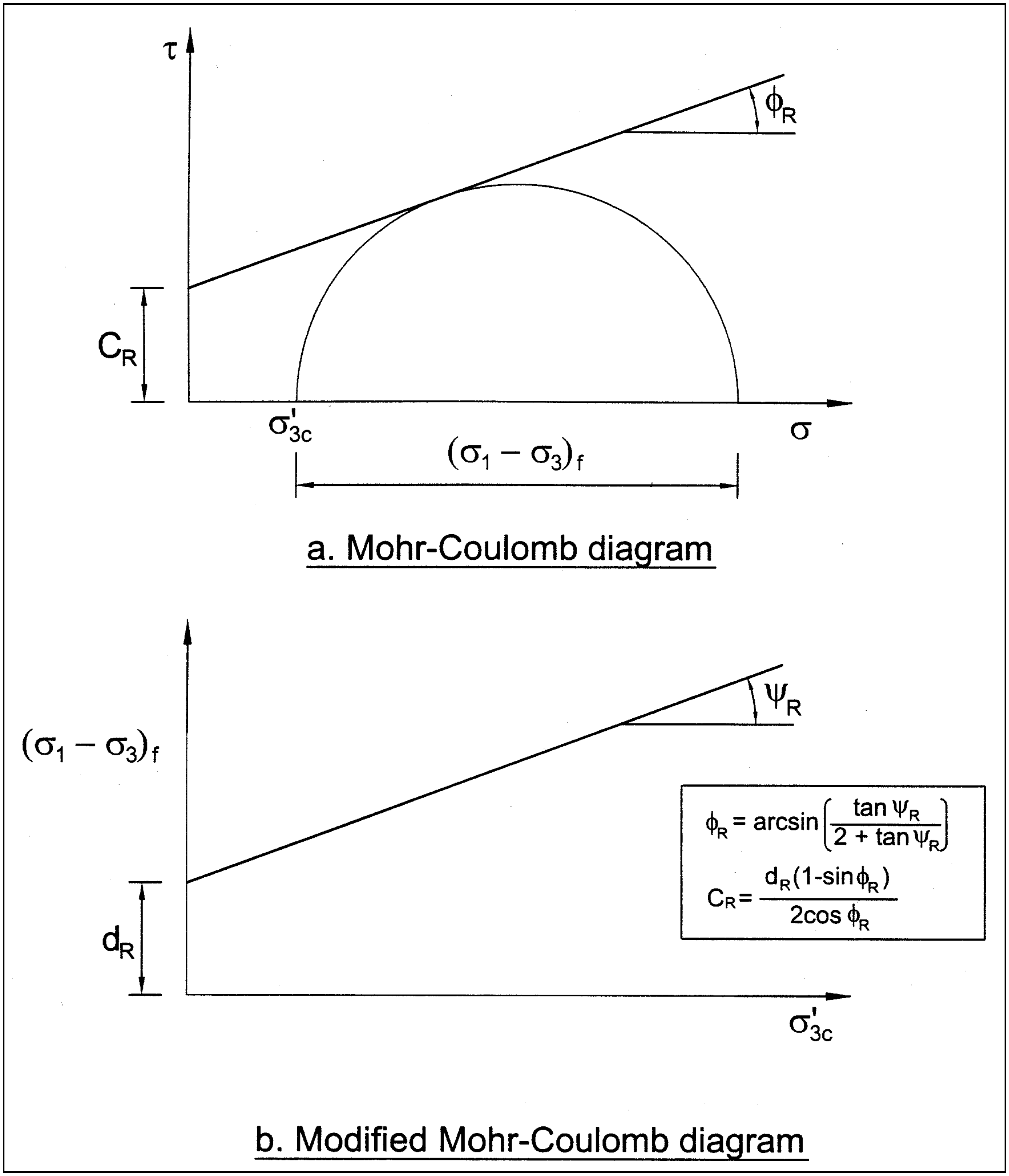


**Figure G-1. R Shear strength envelope used in Corps of Engineers′ (1970) method for rapid drawdown**

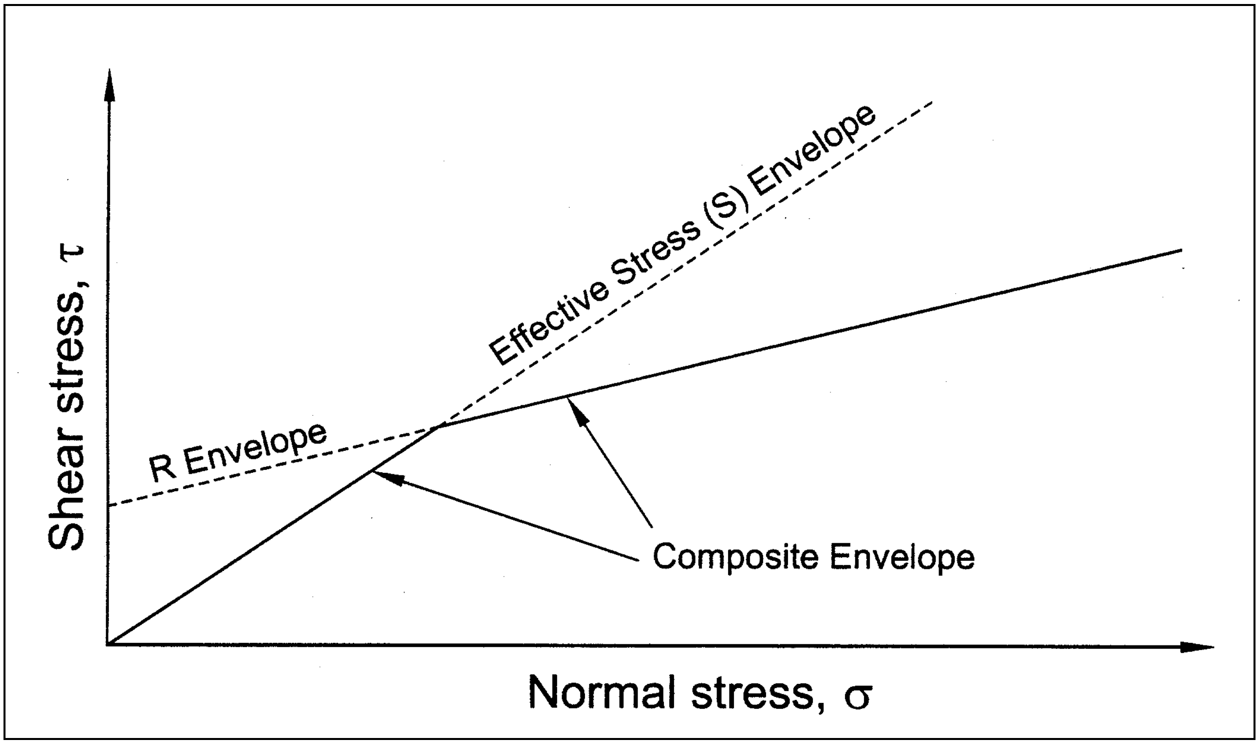


**Figure G-2. Composite shear strength envelope used in Corps of Engineers′ (1970) method for rapid drawdown**

$$\tau_c = \frac{S}{\Delta \ell} \qquad \text{(G-2)}$$

*b. Second-stage shear strengths*. Two shear strength relationships are used to evaluate shear strengths for the second-stage computations.

(1) The first is the relationship between undrained shear strength (shear stress on the failure plane at failure), $\tau_{ff}$, and effective normal stress on the failure plane during consolidation, $\sigma'_{fc}$. This relationship can be determined directly from the results of isotropically consolidated-undrained (CU or R) tests, or it can be calculated from the strength parameters, $c_R$ and $\phi_R$, that are determined from the R envelope shown in Figure G-1.

(a) To determine the relationship between $\tau_{ff}$ and $\sigma'_{fc}$ directly from the results of isotropically consolidated-undrained triaxial compression tests, the shear stress on the failure plane at failure, $\tau_{ff}$, is plotted versus the effective stress on the failure plane at consolidation, $\sigma'_{fc}$. The values of $\tau_{ff}$ and $\sigma'_{fc}$ are calculated using the following equations:

$$\tau_{ff} = \frac{(\sigma_1 - \sigma_3)_f}{2} \cos \phi' \qquad \text{(G-3)}$$

and

$$\sigma'_{fc} = \sigma'_{3c} \qquad \text{(G-4)}$$

where

$(\sigma_1 - \sigma_3)_f$ = principal stress difference at failure

$\phi'$ = effective stress angle of internal friction

$\sigma'_{3c}$ = CU test consolidation pressure

$\sigma'_{fc}$ is equal to $\sigma'_{3c}$ because the consolidation pressure is the same on all planes in an isotropic consolidated undrained triaxial test.

(b) An example relationship of $\tau_{ff}$ vs. $\sigma'_{fc}$ is shown in Figure G-3. The intercept and slope of this envelope are designated, $d_{K_c=1}$ and $\psi_{K_c=1}$. If values of $\tau_{ff}$ and $\sigma'_{fc}$ are determined directly from the CU test results, the values of $d_{K_c=1}$ and $\psi_{K_c=1}$ are determined by drawing a line through the data and measuring the intercept and the slope as indicated in Figure G-3.

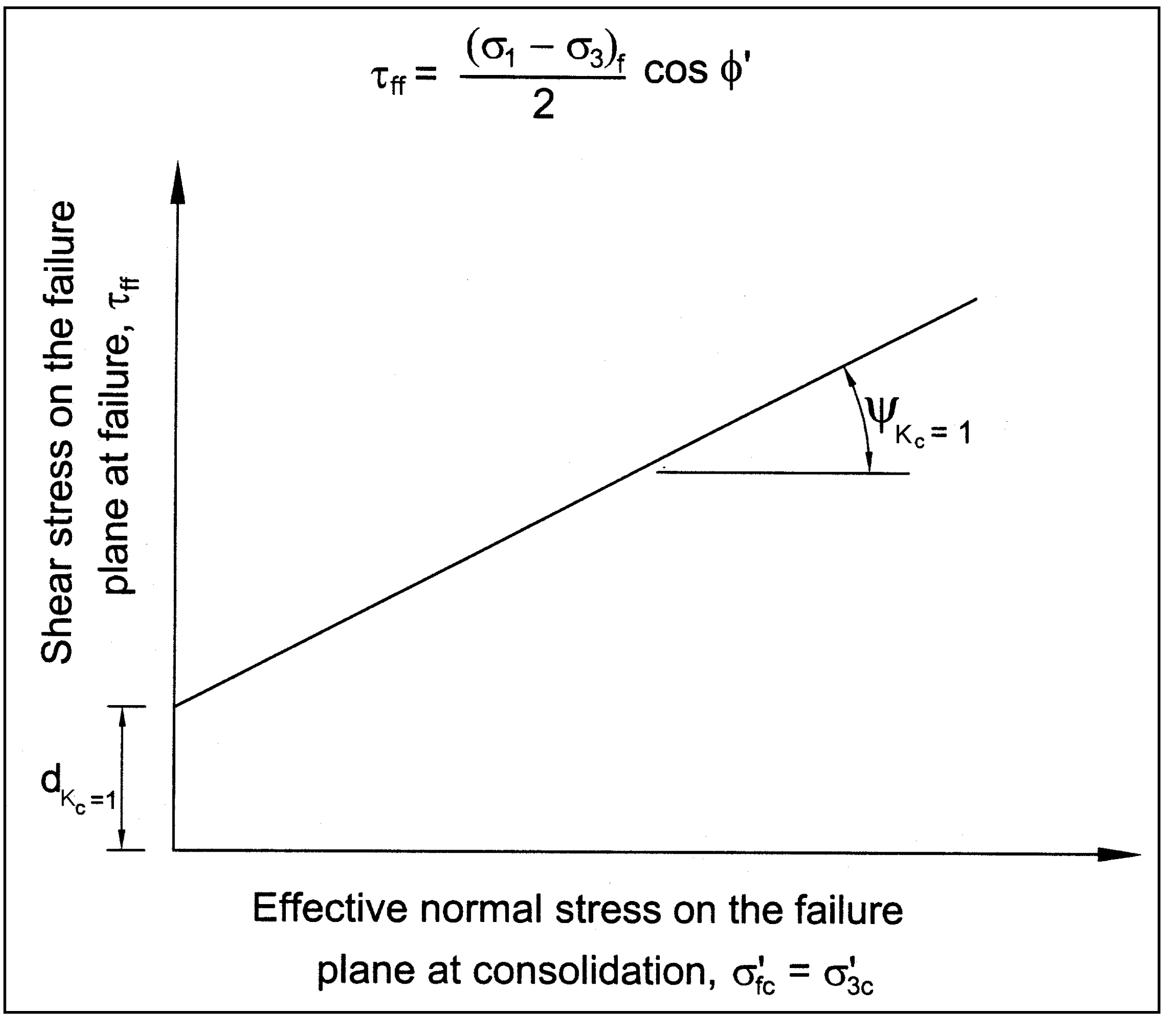


**Figure G-3.** $\tau_{ff}$ **vs** $\sigma'_{fc}$ **Shear strength envelope from isotropically consolidated undrained (CU or R) triaxial compression tests**

(c) The values of $d_{K_c=1}$ and $\psi_{K_c=1}$ are related to the intercept and slope ($c_R$ and $\phi_R$) of the R-envelope shown in Figure G-1 and can be computed if $c_R$ and $\phi_R$ have been evaluated. The relationships between the parameters $d_{K_c=1}$ and $\psi_{K_c=1}$ and the parameters $c_R$ and $\phi_R$ are follows:

$$d_{K_c=1} = c_R \left( \frac{\cos\ \phi_R\ \ \cos\ \phi'}{1 - \sin\ \phi_R} \right) \tag{G-5}$$

$$\psi_{K_c=1} = \tan^{-1} \left( \frac{\sin\ \phi_R\ \ \cos\ \phi'}{1 - \sin\ \phi_R} \right) \tag{G-6}$$

(2) The other shear strength relationship needed for the second-stage computations is the effective stress envelope. Although this envelope is for drained strengths, it may also be viewed as an envelope representing the undrained shear strength of soil that is consolidated to stresses that bring the soil to failure before any undrained loading is applied. In this case, no additional load can be applied in undrained shear before the soil fails. In such a test, the stresses at failure are the same as those at consolidation.

(a) The two shear strength envelopes that are used to determine undrained shear strengths for the second-stage stability computations are shown in Figure G-4. Both envelopes represent relationships between undrained shear strength, $\tau_{ff}$, and effective consolidation pressure on the failure plane, $\sigma'_{fc}$.

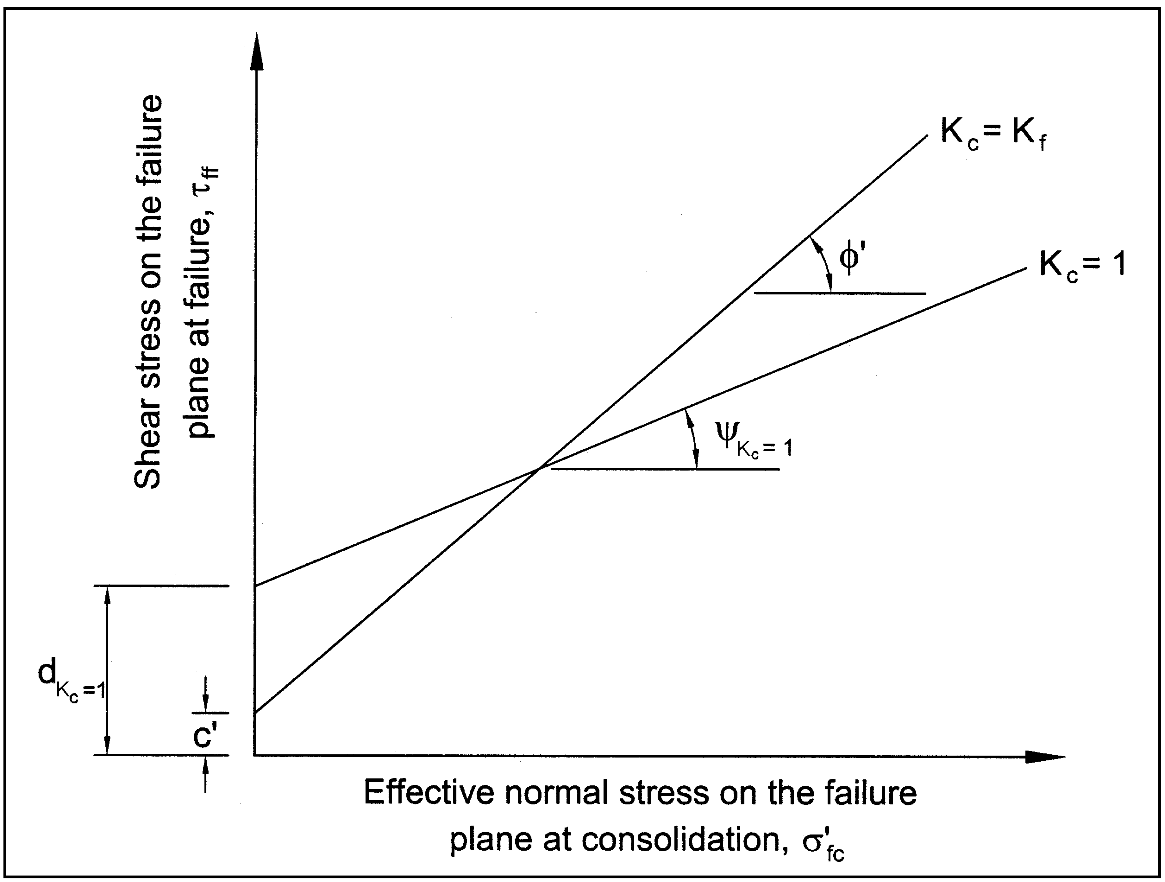


**Figure G-4. $\tau_{ff}$ vs $\sigma'_{fc}$ Shear strength envelope used for improved procedure for rapid drawdown analysis**

(b) The two envelopes shown in Figure G-4 correspond to the extreme possible values of the ratio of $\sigma'_{1c}/\sigma'_{3c} = K_c$. As discussed above, one of the envelopes corresponds to isotropic consolidation, or $K_c = 1$, and the other corresponds to the maximum possible ratio, or $K_c = \sigma'_{1f}/\sigma'_{3f} = K_f$. The undrained shear strengths needed for the second-stage stability analyses are interpolated between these envelopes, using the value of $K_c$ for each slice determined from the first stage computations as the basis for interpolating between the envelopes.

(c) As noted above, the values of $K_c$ ranges from 1.0 to $K_f$. If c' = 0, the value of $K_f$ is given by the following equation:

$$K_f = \frac{1 + \sin\ \phi'}{1 - \sin\ \phi'} \tag{G-7}$$

If c' is not equal to zero, the value of $K_f$ varies with the effective consolidation pressure $\sigma'_{fc}$, as shown by the following equation:

$$K_f = \frac{(\sigma'_{fc} + c'\cos\ \phi')(1 + \sin\ \phi')}{(\sigma'_{fc} - c'\cos\ \phi')(1 - \sin\ \phi')} \tag{G-8}$$

(3) The following steps are used to compute undrained shear strength values for each slice using the stresses $\sigma'_c$ and $\tau_c$ from the first-stage computations:

(a) Compute undrained shear strengths from the two shear strength envelopes shown in Figure G-3. The shear strengths are computed using the effective consolidation stress, $\sigma'_c$, as follows:

$$\tau_{(ff-K_c=1)} = d_{(K_c=1)} + \sigma'_c \tan(\psi_{K_c=1}) \tag{G-9}$$

$$\tau_{(ff-K_c=K_f)} = c' + \sigma'_c \tan(\phi') \tag{G-10}$$

(b) Compute the effective principal consolidation stress ratio at failure, $K_f$, from Equation G-7 or G-8.

(c) Calculate the principal stress ratio at consolidation, $K_c$, for the stresses on the base of the slice,

$$K_c = \frac{\sigma'_c + \tau_c \dfrac{\sin\ \phi' + 1}{\cos\ \phi'}}{\sigma'_c + \tau_c \dfrac{\sin\ \phi' - 1}{\cos\ \phi'}} \tag{G-11}$$

where the stresses $\sigma'_c$ and $\tau_c$ are those from the first-stage computations.

Equation G-11 is derived by assuming that the orientation of the principal stresses during consolidation is the same as at failure, as suggested by Lowe and Karafiath (1960).

(d) Calculate, by linear interpolation between the two values of shear strength determined in Step a, the undrained shear strength, $\tau_{ff}$, for the slice. The undrained shear strength is calculated using the following equation:

$$\tau_{ff} = \frac{(K_f - K_c)\tau_{ff-K_c=1} + (K_c - 1)\tau_{ff-K_c=K_f}}{K_f - 1} \qquad \text{(G-12)}$$

*c. Second-stage computations*. The second-stage computations are performed to calculate stability immediately after drawdown, assuming that all low-permeability materials are undrained. The low-permeability materials are assigned undrained shear strength values calculated from Equation G-12, with $\phi$ set equal to zero. Effective stress shear strength parameters are used for materials that drain freely, and appropriate pore water pressures are prescribed. The pore water pressures for free-draining materials are those after drawdown has occurred and steady-state seepage has been reestablished. The pore water pressures in the low-permeability materials are set equal to zero. If a portion of the slope remains submerged after drawdown, the external water pressures acting on the submerged part of the slope are calculated and applied as external loads to the surface of the slope.

*d. Strengths for third-stage computations.* Once the second-stage computations have been completed, each slice is examined to determine if the drained strength would be less than the undrained strength determined from Equation G-12. The drained shear strength is estimated as follows:

(1) The total normal stress on the base of each slice is calculated by dividing the normal force, N, calculated in the second-stage computations by the length of the base, i.e.,

$$\sigma = \frac{N}{\Delta\ell} \qquad \text{(G-13)}$$

(2) An approximate value of the drained effective stress, $\sigma'_d$, after steady-state seepage is reestablished is computed by subtracting the pore water pressure from the total stress, i.e.,

$$\sigma'_d = \sigma - u \qquad \text{(G-14)}$$

where $\sigma$ is the total normal stress calculated in Equation G-13.

Because the total normal stress is based on the second-stage computations, it is not necessarily the same as the total normal stress that would exist after drainage has occurred. However, it should not be much different, and it is reasonable to assume that it is the same for the purpose of these analyses. The pore water pressure, u, in Equation G-14 should be the pore water pressure after steady-state seepage is reestablished following drawdown. The pore water pressure is not the same as the pore water pressure used in the first-stage computations.

(3) The drained shear strength is estimated using the effective stress calculated in Equation G-14 and the effective stress shear strength parameters, c' and $\phi'$, which are the same as those used in the first-stage computations. The drained shear strength, $s_d$, is calculated from:

$$s_d = c' + \sigma'_d \tan(\phi') \qquad \text{(G-15)}$$

(4) The drained shear strength calculated in Equation G-15 is compared to the value of undrained shear strength for this slice that was used in the second-stage computations. If the drained shear strength is greater than the undrained shear strength for all slices where the undrained shear strength was used previously, then no further computations are required. In that case, the factor of safety after rapid drawdown is equal to the factor of safety calculated for the second stage. If for any slice the drained shear strength is less than the undrained shear strength used for the second-stage computations, a third-stage computation is performed. For

those slices where the drained shear strength is less than the undrained shear strength, the effective stress drained shear strength parameters, c' and $\phi'$, are assigned to those slices for the third-stage computations. Pore water pressures are assigned based on the reestablished steady-state seepage conditions. For those slices where the undrained shear strength is less than the estimated drained shear strength, the same undrained shear strengths used for the second-stage computations are used for the third stage.

*e. Third-stage computations*. The third-stage stability computations are performed using the same conditions as for the second-stage computations, except for those materials where drained strengths are lower than undrained strengths. For those slices the drained strength parameters and appropriate pore water pressures are used, as noted above. The factor of safety after rapid drawdown is equal to the factor of safety calculated for the third stage. If the third-stage computations are not required, the factor of safety after rapid drawdown is equal to the factor of safety calculated for the second stage.

## G-4. Example Problems

Three examples of rapid drawdown stability analyses of the slope shown in Figure G-5 are presented in the following sections. The slope is homogeneous, with the shear strength properties indicated in the table shown in Figure G-5. The unit weight of soil is 135 pcf. The unit weight is assumed to be the same above and below the water levels and does not change as a result of drawdown. Drawdown is from a maximum pool level of 103 feet to a minimum pool of 24 feet.

*a.* All computations are performed for the circular slip surface shown in Figure G-6. The soil mass above the trial slip surface is subdivided into 12 slices. The slip surface is not the critical slip surface.

*b.* For simplicity in the example calculations, it was assumed that the piezometric line was horizontal at the elevation of the maximum pool. Similarly, after drawdown and reestablishment of steady-state seepage, the piezometric line was assumed to be horizontal at the reservoir level after drawdown. In many slopes it would be appropriate to perform seepage analyses to determine the pore water pressures before and after drawdown.

*c.* In the following sections, three analyses are presented. The first uses the Corps of Engineers' 1970 procedure (USACE 1970) for rapid drawdown, and the Modified Swedish Method for the stability calculations. The second uses the improved (and recommended) procedure for rapid drawdown and the Simplified Bishop Method for the stability calculations. The third uses the improved procedure for rapid drawdown, and the Modified Swedish Method for stability calculations, with side force inclinations determined using Spencer's Method.

## G-5. U.S. Army Corps of Engineers' 1970 Procedure - Example

The first analysis uses the U.S. Army Corps of Engineers' 1970 procedure (USACE 1970) for rapid drawdown analyses. Although the improved method described in Section G-3 is recommended, the 1970 method has been used for design of many dams, and it may be necessary to use this method to check those older designs. Stability calculations for the 1970 method were performed using the Modified Swedish Method and the 1970 recommendations regarding the inclination of interslice forces. This was done for consistency with the original procedure as described in the earlier manual, although Spencer's Method is currently recommended. The interslice forces are assumed to be parallel to the average embankment slope. The average embankment slope is 2.84 (horizontal) to 1 (vertical), yielding an interslice force inclination of 19.4 degrees measured from the horizontal.

| Effective stress (CD or S) envelope | | R-envelope | | $\tau_{ff}$ vs. $\sigma'_{fc}$ envelope | |
|---|---|---|---|---|---|
| Intercept, c' | Slope, $\phi'$ | Intercept, $c_R$ | Slope, $\phi_R$ | Intercept, $d_{kc=1}$ | Slope, $\psi_{kc=1}$ |
| 0 | 30° | 1200 psf | 16° | 1379 psf | 18.2° |

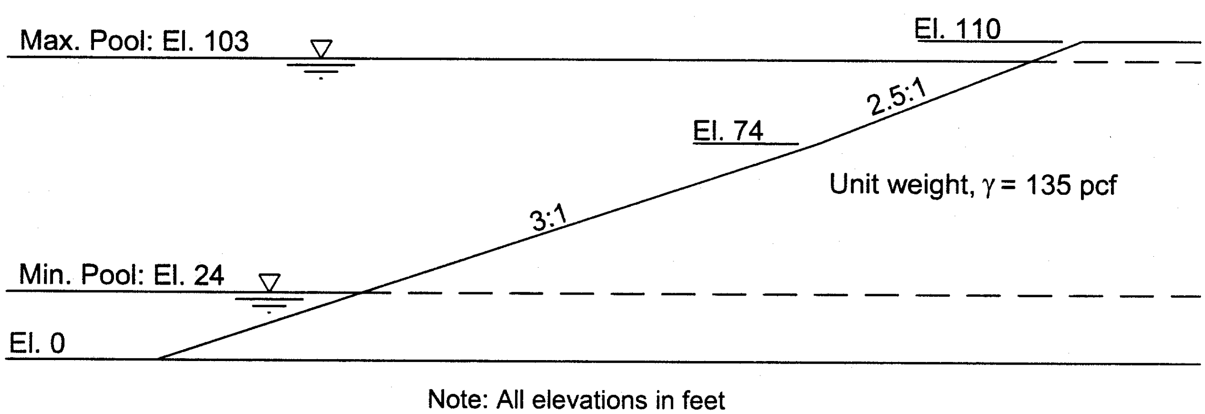


**Figure G-5. Slope and soil properties for example problem**

*a.* The interslice forces are total forces and thus include the water pressures on the sides of the slices. This approach is necessary for the second stage where undrained shear strengths are used and pore water pressures are therefore unknown. For consistency, the same approach was used for both stages. The use of total, rather than effective, interslice forces is also consistent with most computer software. The stability calculations are performed using the numerical Modified Swedish Method. Because undrained shear strengths must be computed from the results of the first-stage analysis, the numerical solution procedures is more suitable than the graphical procedure. Calculations for the numerical procedure are easily performed using spreadsheet software, making the calculations relatively easy as compared with the graphical procedure.

(1) *Step 1 – First-stage computations* Calculations for the first-stage computations are summarized in the table presented in Figure G-7a. Effective stress shear strength parameters (c' = 0, $\phi'$ = 30 degrees) are used for all slices. Slice weights are computed using total unit weight. The pore water pressures are calculated from the horizontal piezometric surface assumed for this example, as explained above.

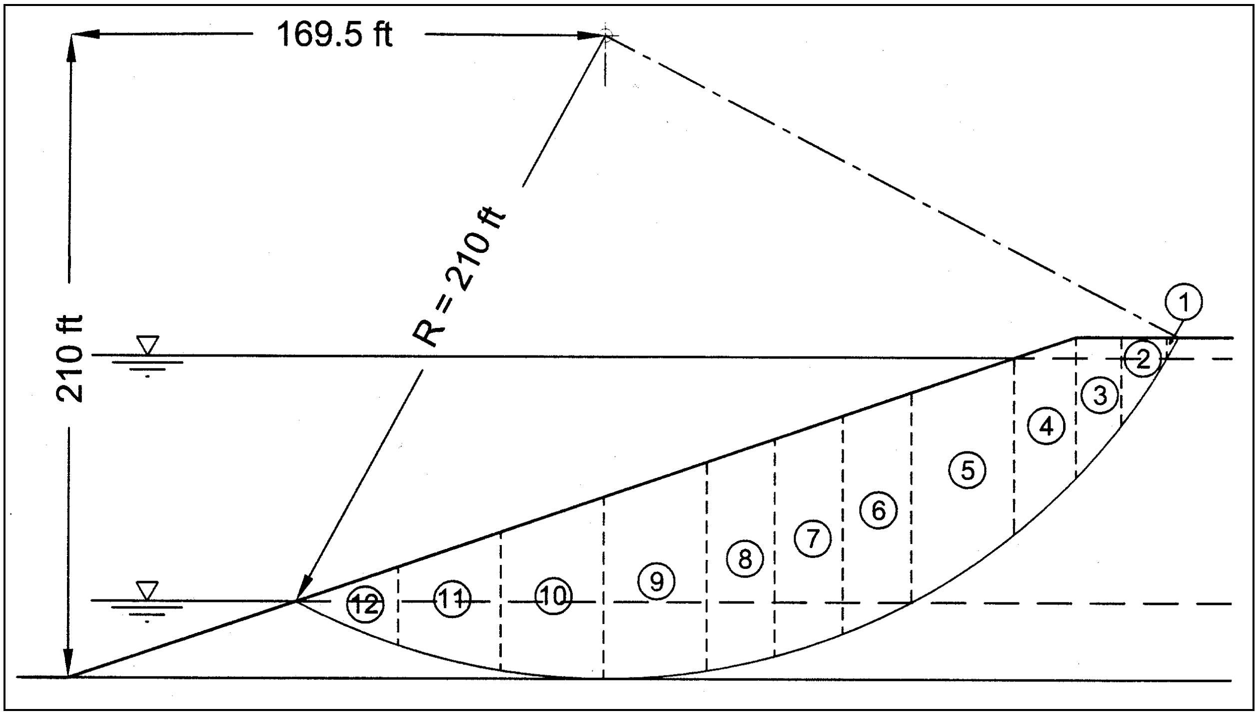


**Figure G-6. Circular slip surface and slices used for computations**

Calculations are shown in Figure G-7a for the final trial value for factor of safety (F = 3.49), which satisfies equilibrium. The factor of safety for the first stage is of little interest. The purpose of the calculations is to determine the stresses on the slip surface for use in computing undrained shear strengths for the second-stage analysis.

(2) *Step 2 – Computation of shear strengths for second-stage analysis*. Calculation of the effective consolidation stress and the shear strengths for the second-stage computations are illustrated in the table shown in Figure G-7b. The steps involved in the computations are as follows:

(a) The total normal force on the base of each slice is calculated using the equation,

$$N = \frac{W + P\cos\beta - (Z_i - Z_{i-1})\sin\theta - (c' - u\ \tan\phi')\dfrac{\Delta\ell}{F}\sin\alpha}{\cos\alpha + \dfrac{\tan\phi'\sin\alpha}{F}} \tag{G-16}$$

The terms in this equation are as defined in Appendix C.

(b) The effective normal stress, $\sigma'_{fc}$, is calculated by dividing the total normal force (N) by the length of the base of the slice, $\Delta\ell$ and subtracting the pore water pressure, i.e.,

$$\sigma'_{fc} = \frac{N}{\Delta\ell} - u \tag{G-17}$$

| 1 | 2 | 3 | 4 | 5 | 6 | 7 | 8 | 9 | 10 | 11 | 12 | 13 | 14 | 15 | 16 | 17 |
|---|---|---|---|---|---|---|---|---|---|---|---|---|---|---|---|---|
| | | | | | Surface loads | | | | | | | | | | | |
| Slice Number | Horizontal Width (b), ft. | Average Slice Height, ft. | Slice Area, sq. ft | Total Weight (W), kips | Height of Surface Water ($h_s$), ft | Press. At Top of Slice ($P_{surface}$), ksf | Slope at Top of Slice ($\beta$), degs | Length of Top of Slice ($\ell_{top}$), ft | Surface Load (P), kips | Base Inclination ($\alpha$), degs. | Slice Base Length ($\ell$), ft. | Piezometric height ($h_p$), ft. | Pore Water Pressure (u), ksf | Cohesion (c), ksf | Friction Angle ($\phi'$), degs. | Interstice Force on Downslope Side ($Z_{i+1}$), kips (Assumed F = 3.49) |
| 1 | 4 | 4 | 14 | 2 | 0 | 0 | 18 | 4 | 0 | 61 | 8 | 0 | 0.00 | 0 | 30 | 2 |
| 2 | 20 | 21 | 428 | 58 | 0 | 0 | 18 | 20 | 0 | 55 | 35 | 14 | 0.89 | 0 | 30 | 53 |
| 3 | 18 | 45 | 807 | 109 | 0 | 0 | 18 | 18 | 0 | 46 | 26 | 38 | 2.36 | 0 | 30 | 132 |
| 4 | 18 | 58 | 1015 | 137 | 0 | 0 | 18 | 19 | 0 | 40 | 23 | 55 | 3.40 | 0 | 30 | 215 |
| 5 | 28 | 65 | 1785 | 241 | 6 | 0.34 | 18 | 30 | 10 | 32 | 32 | 70 | 4.39 | 0 | 30 | 332 |
| 6 | 22 | 69 | 1508 | 204 | 15 | 0.96 | 18 | 24 | 23 | 24 | 24 | 84 | 5.24 | 0 | 30 | 403 |
| 7 | 23 | 68 | 1570 | 212 | 24 | 1.52 | 18 | 25 | 38 | 18 | 24 | 93 | 5.78 | 0 | 30 | 448 |
| 8 | 22 | 66 | 1449 | 196 | 33 | 2.04 | 18 | 23 | 47 | 11 | 22 | 99 | 6.15 | 0 | 30 | 465 |
| 9 | 31 | 60 | 1644 | 249 | 41 | 2.58 | 18 | 32 | 83 | 4 | 31 | 102 | 6.36 | 0 | 30 | 439 |
| 10 | 35 | 49 | 1702 | 230 | 52 | 3.26 | 18 | 36 | 119 | -5 | 35 | 102 | 6.34 | 0 | 30 | 338 |
| 11 | 30 | 34 | 1005 | 136 | 63 | 3.93 | 18 | 32 | 124 | -14 | 31 | 97 | 6.02 | 0 | 30 | 195 |
| 12 | 33 | 12 | 410 | 55 | 73 | 4.59 | 18 | 35 | 159 | -23 | 35 | 86 | 5.36 | 0 | 30 | 10 |

a. First-stage stability computations

| 1 | 2 | 3 | 4 | 5 | 6 |
|---|---|---|---|---|---|
| Total Normal Force (N), kips | Pore Water Pressure (u), ksf | Effective Normal Stress ($\sigma'_{fc}$), ksf | Cohesion (c), ksf | Friction Angle ($\phi$), degrees | $2^{nd}$ Stage Shear Strength ($s_2$), ksf |
| 20 | 0 | 0.25 | 0 | 30 | 1.47 |
| 63 | 0.89 | 0.92 | 0 | 30 | 0.53 |
| 111 | 2.36 | 1.9 | 0 | 30 | 1.1 |
| 134 | 3.4 | 2.51 | 0 | 30 | 1.45 |
| 240 | 4.39 | 2.99 | 0 | 30 | 1.73 |
| 214 | 5.24 | 3.64 | 0 | 30 | 2.1 |
| 238 | 5.78 | 4.08 | 0 | 30 | 2.35 |
| 236 | 6.15 | 4.38 | 1.2 | 16 | 2.46 |
| 336 | 6.36 | 4.62 | 1.2 | 16 | 2.53 |
| 379 | 6.34 | 4.61 | 1.2 | 16 | 2.52 |
| 315 | 6.02 | 4.18 | 1.2 | 16 | 2.4 |
| 302 | 5.36 | 3.08 | 0 | 30 | 1.78 |

b. Strength computations for second stage

**Figure G-7. Computations with Corps of Engineers' (1970) method – first stage**

(c) The shear strength, $s_2$, for the second-stage computations is calculated using the composite shear strength envelope shown in Figure G-8. This envelope is the lower bound envelope derived from the R and S envelopes. The shear strength, $s_2$, is calculated using the composite envelope and the effective consolidation pressure, $\sigma'_c$, determined in Step 2. For the example calculations shown in Figure G-7b, the effective normal stress, $\sigma'_{fc}$, shown in Column 3 was first compared with the effective stress, $\tau_{ff}$ and $\sigma_i$, corresponding to the point where the R and S envelopes intersect. The stress where the two envelopes intersect is given by:

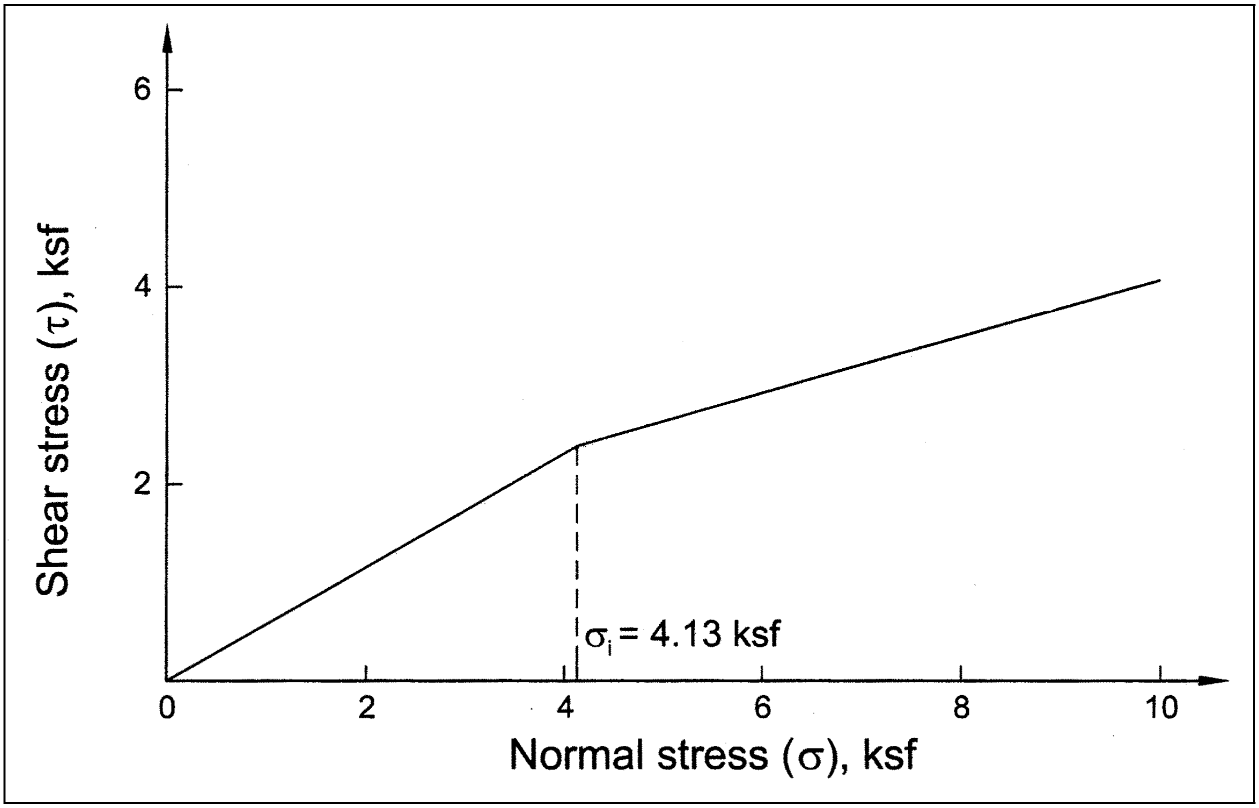


**Figure G-8. Composite shear strength envelope for example problem – Corps of Engineers' (1970) method**

$$\sigma_i = \frac{c_R - c_S}{\tan\ \phi_S - \tan\ \phi_R} \tag{G-18}$$

(d) For the example problem, the two envelopes intersect at $\sigma_i = 4.13$ ksf. If the effective stress, $\sigma'_c$, is less than $\sigma_i$, the effective stress shear strength parameters (c' and $\phi'$) are used to compute the strength, $s_2$. Otherwise, the R envelope parameters ($c_R$ and $\phi_R$) are used (Columns 4 and 5 of table in Figure G-7b). The shear strength was computed from the relationship:

$$s_2 = c + \sigma'_c \tan(\phi) \tag{G-19}$$

where c and $\phi$ are the appropriate values shown in Columns 4 and 5 in Figure G-7b.

The shear strengths are shown in Column 6 of the table in Figure G-7b.

(3) *Step 3 – Second-stage computations*. Calculations for the second stage are shown in the table presented in Figure G-9. The specific details of the computations shown in Figure G-9 are as follows:

(a) The slice weight is calculated using the total unit weights after drawdown. In this example, the soil is assumed to be saturated before and after drawdown. Thus the total unit weights and the weights of the slices are the same as for the first stage. This will not always be the case.

(b) Because the reservoir is below the top of the lowest slice after drawdown, the surface loads (P) are zero. In other cases the surface loads may not be zero.

| 1 | 2 | 3 | 4 | 5 | 6 | 7 | 8 | 9 | 10 | 11 | 12 | 13 | 14 | 15 |
|---|---|---|---|---|---|---|---|---|---|---|---|---|---|---|
| | | | Surface Loads | | | | | | | | | | | |
| Slice Number. | Slice Area, sq. ft. | Total Weight (W), kips. | Height of Surface Water ($h_s$), ft. | Press. At Top of Slice ($P_{surface}$), ksf | Slope at Top of Slice ($\beta$), degs | Length of Top of Slice ($\ell_{top}$), ft | Surface Load (P), kips | Base Inclination ($\alpha$), degs. | Slice Base Length ($\ell$), ft. | Piezometric height ($h_p$), ft. | Pore Water Pressure (u), ksf | Cohesion (c), ksf | Friction Angle ($\phi'$), degs. | Interstice Force on Downslope Side ($Z_{i+1}$), kips (Assumed F = 1.35) |
| 1 | 14 | 2 | 0 | 0 | 18 | 4 | 0 | 61 | 8 | 0 | 0 | 0.15 | 0 | 1 |
| 2 | 428 | 58 | 0 | 0 | 18 | 20 | 0 | 55 | 35 | 0 | 0 | 0.53 | 0 | 42 |
| 3 | 807 | 109 | 0 | 0 | 18 | 18 | 0 | 46 | 26 | 0 | 0 | 1.1 | 0 | 106 |
| 4 | 1015 | 137 | 0 | 0 | 18 | 19 | 0 | 40 | 23 | 0 | 0 | 1.45 | 0 | 174 |
| 5 | 1785 | 241 | 0 | 0 | 18 | 30 | 0 | 32 | 32 | 0 | 0 | 1.73 | 0 | 262 |
| 6 | 1508 | 204 | 0 | 0 | 18 | 24 | 0 | 24 | 24 | 0 | 0 | 2.1 | 0 | 309 |
| 7 | 1570 | 212 | 0 | 0 | 18 | 25 | 0 | 18 | 24 | 0 | 0 | 2.35 | 0 | 331 |
| 8 | 1449 | 196 | 0 | 0 | 18 | 23 | 0 | 11 | 22 | 0 | 0 | 2.46 | 0 | 329 |
| 9 | 1844 | 249 | 0 | 0 | 18 | 32 | 0 | 4 | 31 | 0 | 0 | 2.53 | 0 | 288 |
| 10 | 1702 | 230 | 0 | 0 | 18 | 36 | 0 | -5 | 35 | 0 | 0 | 2.52 | 0 | 197 |
| 11 | 1005 | 136 | 0 | 0 | 18 | 32 | 0 | -14 | 31 | 0 | 0 | 2.4 | 0 | 93 |
| 12 | 410 | 55 | 0 | 0 | 18 | 35 | 0 | -23 | 35 | 0 | 0 | 1.78 | 0 | 0 |

**Figure G-9. Computations with Corps of Engineers' (1970) method – second stage**

(c) The shear strengths ($s_2$) calculated in Step 2 are assigned as values of cohesion (c) and $\phi$ is set equal to zero. Pore water pressures are not relevant because $\phi$ is equal to zero. If the bases of some slices had been located in soils that drain freely, effective stress shear strength parameters (c' and $\phi'$) and appropriate pore water pressures would have been assigned to those slices for the second-stage computations. The pore water pressures in the freely draining soils would be those following drawdown.

(d) The side forces, $Z_{i+1}$, shown in Figure G-9 are the final values calculated using the value of the factor of safety that satisfies force equilibrium. Equilibrium is confirmed by the negligible force on the right side of the last slice (slice 12). The factor of safety computed for the second-stage analyses is 1.35. This value is the factor of safety after rapid drawdown for the assumed slip surfaces. It would be necessary to analyze additional slip surfaces to determine the critical surface and the lowest factor of safety.

## G-6. Improved Method for Rapid Drawdown – Example Calculations with Simplified Bishop Method

*a. First-stage computations*. Calculations for the first stage of the computations are summarized in the table presented in Figure G-10a. The calculations follow the same steps and procedure described in section F.2.b for steady seepage analyses. Effective stress shear strength parameters (c' = 0, $\phi'$ = 30 degrees) are used for all slices. Slice weights are computed using total unit weights. The pore water pressures and external water loads are calculated from the maximum pool piezometric surface shown in Figure G-5. Calculations are shown in Figure G-10 for the final trial value of the factor of safety (F = 2.20).

*b. Calculation of shear strengths for second-stage computations*. Calculations of the consolidation stresses and undrained shear strengths for the second stage of the computations are presented in the table in Figure G-10b. The specific steps involved are as follows:

(1) The total normal force on the base of each slice is calculated using the equation:

$$N = \frac{W + P\cos\beta - \frac{1}{F}\left[(c' - u\tan\phi')\, b\tan\alpha\right]}{\left(\cos\alpha + \frac{\sin\alpha\tan\phi'}{F}\right)} \qquad \text{(G-20)}$$

where the terms are as defined previously. The values for all quantities are from the first-stage computations.

(2) Pore water pressures, u, are determined from the initial condition with the piezometric level at elevation 103 ft (Column 2 in Figure G-7b). These pore water pressures are the same as the ones used for the first-stage computations (Column 16 in Figure G-7a).

(3) The effective normal stress, $\sigma'_c$, is calculated by dividing the total normal force (N) by the length of the base of the slice, $\Delta\ell$, and subtracting the pore water pressure:

$$\sigma'_c = \frac{N}{\Delta\ell} - u \qquad \text{(G-21)}$$

(4) The shear force (S) on the base of the slice is calculated from the equation:

| 1 | 2 | 3 | 4 | 5 | 6 | 7 | 8 | 9 | 10 | 11 | 12 | 13 | 14 | 15 | 16 | 17 | 18 | 19 | 20 | 21 |
|---|---|---|---|---|---|---|---|---|---|---|---|---|---|---|---|---|---|---|---|---|
| | | | | | | | Surface loads | | | | | | | | | | | | | |
| Slice Number | Horizontal Width (b), ft. | Average Slice Height, ft. | Slice Area, sq. ft | Total Weight (W), kips | Base Inclination ($\alpha$), degs. | W sin ($\alpha$), kips. | Height of Surface ater ($h_s$), ft. | Avg. Surface Press. ($P_{surface}$), ksf. | Surface Inclination ($\beta$), degs. | Surface Load (P), kips. | Horiz. Moment arm ($d_h$), ft. | Vert. Moment arm ($d_v$), ft. | Moment ($M_p$), kip-ft. | Piezometric Height ($h_p$), ft. | Pore Water Pressure (u), ksf | Cohesion (c), ksf | Friction Angle ($\phi'$), degs. | $c'b + (W + P\cos\beta - ub)\tan\phi'$ | $m_\alpha$ (Assumed F = 2.20) | $[c'b + (W + P\cos\beta - ub)\tan\phi'] \div m_\alpha$ |
| 1 | 4 | 4 | 14 | 2 | 61 | 2 | 0 | 0 | 0 | 0 | - | - | - | 0 | 0 | 0 | 30 | 1 | 0.72 | 1 |
| 2 | 20 | 21 | 428 | 58 | 55 | 47 | 0 | 0 | 0 | 0 | - | - | - | 14 | 0.89 | 0 | 30 | 23 | 0.79 | 29 |
| 3 | 18 | 45 | 807 | 109 | 46 | 79 | 0 | 0 | 0 | 0 | - | - | - | 38 | 2.36 | 0 | 30 | 38 | 0.88 | 44 |
| 4 | 18 | 58 | 1015 | 137 | 40 | 87 | 0 | 0 | 21.8 | 0 | - | - | - | 55 | 3.4 | 0 | 30 | 45 | 0.94 | 48 |
| 5 | 28 | 65 | 1785 | 241 | 32 | 128 | 6 | 0.34 | 21.8 | 10 | -111 | 113 | -626 | 70 | 4.39 | 0 | 30 | 75 | 0.99 | 76 |
| 6 | 22 | 69 | 1508 | 204 | 24 | 84 | 15 | 0.96 | 21.8 | 23 | -86 | 122 | -793 | 84 | 5.24 | 0 | 30 | 63 | 1.02 | 62 |
| 7 | 23 | 68 | 1570 | 212 | 18 | 65 | 24 | 1.52 | 21.8 | 38 | -64 | 131 | -401 | 93 | 5.78 | 0 | 30 | 66 | 1.03 | 64 |
| 8 | 22 | 66 | 1449 | 196 | 11 | 39 | 33 | 2.04 | 18.4 | 47 | -42 | 140 | 227 | 99 | 6.15 | 0 | 30 | 61 | 1.03 | 59 |
| 9 | 31 | 60 | 1844 | 249 | 4 | 18 | 41 | 2.58 | 18.4 | 83 | -15 | 148 | 2698 | 102 | 6.36 | 0 | 30 | 77 | 1.02 | 76 |
| 10 | 35 | 49 | 1702 | 230 | -5 | -19 | 52 | 3.26 | 18.4 | 119 | 17 | 159 | 7911 | 102 | 6.34 | 0 | 30 | 71 | 0.98 | 73 |
| 11 | 30 | 34 | 1005 | 136 | -14 | -32 | 63 | 3.93 | 18.4 | 124 | 50 | 170 | 12521 | 97 | 6.02 | 0 | 30 | 42 | 0.91 | 46 |
| 12 | 33 | 12 | 410 | 55 | -23 | -21 | 73 | 4.59 | 18.4 | 159 | 81 | 180 | 21358 | 86 | 5.36 | 0 | 30 | 17 | 0.82 | 21 |
| | | | | | | 476 | | | | | | | 42895 | | | | | | | 599 |

$$F = \frac{599}{476 - \frac{42895}{210}} = 2.20$$

a. First-stage stability computations

| 1 | 2 | 3 | 4 | 5 | 6 | 7 | 8 | 9 | 10 |
|---|---|---|---|---|---|---|---|---|---|
| Total Normal Force (N), kips | Pore Water Pressure (u), ksf | Effective Normal Stress ($\sigma'_c$), ksf | Shear Force (S), kips | Shear Stress ($\tau_{fc}$), ksf | Consolidation Stress Ratio ($K_c$) | $\tau_{ff}$ ($K_c$ = 1), ksf | $\tau_{ff}$ ($K_c = K_f$), ksf | Effective Prin. Stress Ratio at Failure, $K_f$ | Interpolated Strength ($\tau_{ff}$), ksf |
| 3 | 0 | 0.32 | 1 | 0.08 | 1.71 | 1.49 | 0.19 | 3.00 | 1.02 |
| 81 | 0.89 | 1.44 | 13 | 0.38 | 1.71 | 1.85 | 0.83 | 3.00 | 1.49 |
| 137 | 2.36 | 2.9 | 20 | 0.76 | 1.71 | 2.33 | 1.67 | 3.00 | 2.1 |
| 160 | 3.4 | 3.64 | 22 | 0.95 | 1.71 | 2.58 | 2.1 | 3.00 | 2.41 |
| 274 | 4.39 | 4.05 | 34 | 1.06 | 1.71 | 2.71 | 2.34 | 3.00 | 2.58 |
| 234 | 5.24 | 4.45 | 28 | 1.17 | 1.71 | 2.84 | 2.57 | 3.00 | 2.75 |
| 250 | 5.78 | 4.57 | 29 | 1.2 | 1.71 | 2.88 | 2.64 | 3.00 | 2.8 |
| 240 | 6.15 | 4.54 | 27 | 1.19 | 1.71 | 2.87 | 2.62 | 3.00 | 2.78 |
| 326 | 6.36 | 4.31 | 35 | 1.13 | 1.71 | 2.8 | 2.49 | 3.00 | 2.69 |
| 346 | 6.34 | 3.66 | 33 | 0.96 | 1.71 | 2.58 | 2.11 | 3.00 | 2.42 |
| 266 | 6.02 | 2.6 | 21 | 0.68 | 1.71 | 2.23 | 1.5 | 3.00 | 1.97 |
| 228 | 5.36 | 1.01 | 10 | 0.27 | 1.71 | 1.71 | 0.59 | 3.00 | 1.31 |

b. Strength computations for second stage

Figure G-10. Computations with improved drawdown procedure – Simplified Bishop Method – first stage

$$S = \frac{1}{F}\left[\frac{c'b + (W + P\ \cos\ \beta - ub)\ \tan\ \phi'}{\cos\alpha + \frac{\sin\alpha\ \tan\phi'}{F}}\right] \tag{G-22}$$

where the values for all quantities are from the first stage analysis.

(5) The shear stress, $\tau_c$, during consolidation is calculated by dividing the shear force (S) by the length of the base of the slice, $\Delta\ell$:

$$\tau_c = \frac{S}{\Delta\ell} \tag{G-23}$$

(6) The effective principal stress ratio for consolidation, $K_c$, is calculated for each slice using the equation:

$$K_c = \frac{\sigma'_c + \tau_c\ \frac{\sin\phi' + 1}{\cos\phi'}}{\sigma'_c + \tau_c\ \frac{\sin\phi' - 1}{\cos\phi'}} \tag{G-24}$$

where $\sigma'_c$ and $\tau_c$ are the values calculated in Steps 3 and 5 above, and $\phi'$ is the effective stress friction angle.

(7) Undrained shear strengths, expressed as the shear stresses on the failure plane at failure, $\tau_{ff\text{-}K_c=1}$ and $\tau_{ff\text{-}K_c=K_f}$, are calculated from the $\tau_{ff}$ vs. $\sigma'_{fc}$ shear strength envelopes for $K_c = 1$ and $K_c = K_f$, respectively (Columns 7 and 8 in Figure G-10b).

(8) The effective principal stress ratio at failure, $K_f$, is calculated from:

$$K_f = \frac{(\sigma'_c + c'\ \cos\ \phi')(1 + \sin\phi')}{(\sigma'_c - c'\ \cos\phi')(1 - \sin\phi')} \tag{G-25}$$

or, when c' = 0:

$$K_f = \frac{1 + \sin\phi'}{1 - \sin\phi'} = \tan^2\left(45° + \frac{\phi'}{2}\right) \tag{G-26}$$

(9) Undrained shear strengths, $\tau_{ff}$, are computed by linear interpolation between the values of shear strength from the $K_c = 1$ envelope and the $K_c = K_f$ envelopes:

$$\tau_{ff} = \frac{(K_f - K_c)\tau_{ff-K_c=1} + (K_c - 1)\tau_{ff-K_c=K_f}}{K_f - 1} \tag{G-27}$$

These undrained shear strengths are used for the second-stage computations.

*c. Second-stage computations.* Calculations for the second stage are shown in the table in Figure G-11a. The specific details of the computations shown in Figure G-11a are as follows:

(1) The slice weight is calculated using the total unit weights after drawdown.

(2) Because the reservoir is below the top of the lowest slice after drawdown, the surface loads (P) are zero. In other cases, the surface loads may not be zero.

(3) The shear strengths computed in Step 2 are assigned as values of cohesion (c), and $\phi$ is set equal to zero. Pore water pressures are not relevant because $\phi$ is zero. If the base of some slices had been located in soils that drain freely, effective stress, shear strength parameters (c' and $\phi'$), and appropriate pore water pressures would be assigned to those slices for the second-stage computations. The pore water pressures in the freely draining soils would be those following drawdown.

(4) The stability calculations in Figure G-11a for the second-stage are shown for the final value of the factor of safety (F = 1.52), where the assumed and calculated values are equal.

*d. Evaluation of strengths for third-stage analyses.* The drained strengths of the soil are calculated as shown in Figure G-11b. The specific steps are as follows:

(1) The total normal force on the base of each slice is calculated from Equation G-16. The values of the quantities in this equation are from the second-stage computations. For slices that were considered to be freely draining, effective stress, shear strength parameters and second-stage pore water pressures are used. For slices that were assumed to be undrained, the value of c in Equation G-19 is the undrained shear strength and $\phi$ is set equal to zero.

(2) The pore water pressures, u, after drawdown are calculated from the final reservoir level.

(3) The effective normal stress, $\sigma'_d$, is calculated using the normal forces and pore water pressures calculated in Steps 1 and 2, and the following equation:

$$\sigma'_d = \frac{N}{\Delta\ell} - u \tag{G-28}$$

(4) The drained shear strength is estimated from:

$$s_d = c' + \sigma'_d \tan(\phi') \tag{G-29}$$

where c' and $\phi'$ are the effective stress shear strength parameters.

(5) The drained shear strengths calculated in Step 4 are compared with the undrained shear strengths, $\tau_{ff}$, used in the second-stage computations to determine which is lower. If the drained shear strength ($s_d$) is lower for any slice, a third-stage of computations is required. In this case, effective stress shear strength parameters, c' and $\phi'$, are used for slices where the drained shear strengths are lower, and undrained shear strengths are used for the slices where the undrained strengths are lower. The undrained shear strengths used are the same as for the second-stage computations. If the undrained shear strengths are lower than the drained strengths for all slices, the undrained shear strengths are more critical and the third-stage computations are not required. In this case, the factor of safety for rapid drawdown is the factor of safety calculated for the second stage.

| 1 | 2 | 3 | 4 | 5 | 6 | 7 | 8 | 9 | 10 | 11 | 12 | 13 | 14 | 15 | 16 | 17 | 18 | 19 |
|---|---|---|---|---|---|---|---|---|---|---|---|---|---|---|---|---|---|---|
| | | | | | Surface loads | | | | | | | | | | | | | |
| Slice Number. | Slice Area, sq. ft. | Total Weight (W), kips. | Base Inclination (α), degs. | W sin (α), kips. | Height of Surface Water ($h_s$), ft. | Avg. Surface Press. ($P_{surface}$), ksf. | Surface Inclination (β), degs. | Surface Load (P), kips. | Horiz. Moment arm ($d_h$), ft. | Vert. Moment arm ($d_v$), ft. | Moment ($M_p$), kip-ft. | Piezometric Height ($h_p$), ft. | Pore Water Pressure (u), ksf | Cohesion (c), ksf | Friction Angle (φ'), degs. | c'b + (W + P cos β - ub) tan φ' | $m_\alpha$ (Assumed F = 1.52) | [c'b + (W + P cos β - ub) tan φ'] ÷ $m_\alpha$ |
| 1 | 14 | 2 | 61 | 2 | 0 | 0 | 0 | 0 | - | - | 0 | - | 0 | 1.02 | 0 | 4 | 0.49 | 8 |
| 2 | 428 | 58 | 55 | 47 | 0 | 0 | 0 | 0 | - | - | 0 | - | 0 | 1.49 | 0 | 30 | 0.58 | 52 |
| 3 | 807 | 109 | 46 | 79 | 0 | 0 | 0 | 0 | - | - | 0 | - | 0 | 2.10 | 0 | 38 | 0.69 | 55 |
| 4 | 1015 | 137 | 40 | 87 | 0 | 0 | 21.8 | 0 | - | - | 0 | - | 0 | 2.41 | 0 | 42 | 0.77 | 55 |
| 5 | 1785 | 241 | 32 | 128 | 0 | 0 | 21.8 | 0 | - | - | 0 | - | 0 | 2.58 | 0 | 71 | 0.85 | 84 |
| 6 | 1508 | 204 | 24 | 84 | 0 | 0 | 21.8 | 0 | - | - | 0 | - | 0 | 2.75 | 0 | 60 | 0.91 | 66 |
| 7 | 1570 | 212 | 18 | 65 | 0 | 0 | 21.8 | 0 | - | - | 0 | - | 0 | 2.80 | 0 | 64 | 0.95 | 68 |
| 8 | 1449 | 196 | 11 | 39 | 0 | 0 | 18.4 | 0 | - | - | 0 | - | 0 | 2.78 | 0 | 61 | 0.98 | 62 |
| 9 | 1844 | 249 | 4 | 18 | 0 | 0 | 18.4 | 0 | - | - | 0 | - | 0 | 2.69 | 0 | 82 | 1.00 | 82 |
| 10 | 1702 | 230 | -5 | -19 | 0 | 0 | 18.4 | 0 | - | - | 0 | - | 0 | 2.42 | 0 | 83 | 1.00 | 84 |
| 11 | 1005 | 136 | -14 | -32 | 0 | 0 | 18.4 | 0 | - | - | 0 | - | 0 | 1.97 | 0 | 59 | 0.97 | 61 |
| 12 | 410 | 55 | -23 | -21 | 0 | 0 | 18.4 | 0 | - | - | 0 | - | 0 | 1.31 | 0 | 43 | 0.92 | 47 |
| | | | | 476 | | | | | | | 0 | | | | | | | 723 |

$$F = \frac{723}{476 - \frac{0}{210}} = 1.52$$

a. Second-stage stability computations

| 1 | 2 | 3 | 4 | 5 | 6 | 7 |
|---|---|---|---|---|---|---|
| Total Normal Force (N), kips | Piezometric Height ($h_p$), ft. | "Drained" Pore Pressure (u), ft | Drained Effective Stress ($\sigma'_{drained}$), ksf | Undrained Shear Strength ($\tau_{ff}$), ksf | Drained Shear Strength ($S_{drained}$), ksf | Strength for Third Stage* |
| -6 | 0 | 0 | -0.72 | 1.02 | 0 | D |
| 52 | 0 | 0 | 1.48 | 1.49 | 0.86 | D |
| 120 | 0 | 0 | 4.61 | 2.1 | 2.66 | U |
| 148 | 0 | 0 | 6.52 | 2.41 | 3.76 | U |
| 250 | 0 | 0 | 7.69 | 2.58 | 4.44 | U |
| 204 | 5 | 0.31 | 8.13 | 2.75 | 4.69 | U |
| 208 | 14 | 0.85 | 7.77 | 2.8 | 4.49 | U |
| 191 | 20 | 1.22 | 7.3 | 2.78 | 4.22 | U |
| 246 | 23 | 1.43 | 6.61 | 2.69 | 3.81 | U |
| 235 | 23 | 1.41 | 5.38 | 2.42 | 3.11 | U |
| 149 | 18 | 1.09 | 3.75 | 1.97 | 2.16 | U |
| 73 | 7 | 0.43 | 1.61 | 1.31 | 0.93 | D |

b. Strength computations for third stage

| 1 | 2 | 3 | 4 | 5 | 6 |
|---|---|---|---|---|---|
| Pore Water Pressure (u), ksf | Cohesion (c), ksf | Friction Angle (φ'), degs. | c'b + (W + P cos β - ub) tan φ' | $m_\alpha$ (Assumed F = 1.44) | [c'b + (W + P cos β - ub) tan φ'] ÷ $m_\alpha$ |
| 0 | 0 | 30 | 1 | 0.84 | 1 |
| 0 | 0 | 30 | 33 | 0.91 | 37 |
| 0 | 2.1 | 0 | 38 | 0.69 | 55 |
| 0 | 2.41 | 0 | 42 | 0.77 | 55 |
| 0 | 2.58 | 0 | 71 | 0.85 | 84 |
| 0 | 2.75 | 0 | 60 | 0.91 | 66 |
| 0 | 2.8 | 0 | 64 | 0.95 | 68 |
| 0 | 2.78 | 0 | 61 | 0.98 | 62 |
| 0 | 2.69 | 0 | 82 | 1.00 | 82 |
| 0 | 2.42 | 0 | 83 | 1.00 | 84 |
| 0 | 1.97 | 0 | 59 | 0.97 | 61 |
| 0.43 | 0 | 30 | 24 | 0.77 | 31 |
| | | | | | 685 |

$$F = \frac{685}{476 - \frac{0}{210}} = 1.44$$

c. Third-stage stability computations

Figure G-11. Computations with improved drawdown procedure – Simplified Bishop Method – second and third stages *e. Third-stage computations*. For the example problem, the drained strengths are lower than the undrained strengths for slices 1, 2, and 12. Therefore, third-stage computations are required. The third-stage computations are shown in the table in Figure G-11c. For the third-stage computations, the conditions are the same as those for the second stage except for the shear strength parameters and the pore water pressures assigned to slices 1, 2, and 12, where the drained shear strengths were determined to be lower. For these slices the pore water pressures are calculated from the piezometric surface at el 24 feet. For all other slices, the undrained shear strengths used for the second-stage computations are also used for the third-stage computations. Pore water pressures were set equal to zero for slices where undrained shear strengths are used. There were no external water loads for the second- or third-stage computations, because the water level was below the top of the last slice after drawdown.

The third-stage computations are summarized in Figure G-11c for the final trial value of the factor of safety, F = 1.44. This value is the factor of safety after rapid drawdown for this method.

## G-7. Improved Procedure for Rapid Drawdown – Example Calculations with Modified Swedish/Spencer Procedure

This example uses the improved procedure for rapid drawdown analysis and the Modified Swedish Method. In these calculations, the inclination of the interslice forces was determined by first computing the factor of safety using Spencer's Method. Thus, the factors of safety computed are identical to those calculated by Spencer's Method. These calculations are the type of calculations that would be performed to check the results of an analysis performed using Spencer's Method. When this procedure is used for analysis, the recommended procedure for checking the calculations is to use the Modified Swedish Method with the interslice force inclination computed in the analysis with Spencer's Method.

The interslice force inclinations determined for Spencer's Method are different for each of the three stages. The interslice force inclinations from Spencer's analysis are summarized in the tabulation below:

| Stage | Interslice Force Inclination (degrees) |
|---|---|
| 1 | 6.0 |
| 2 | 12.2 |
| 3 | 13.7 |

*a. First-stage computations*. Calculations for the first stage of the computations are summarized in the table in Figure G-12a. Except for differences resulting from the assumed interslice force inclination, the quantities shown in Figure G-12a are the same as those shown previously for the first-stage computations with the Corps of Engineers' (1970a) method, described in Section G-5a. Refer to Section G-5 for discussion of shear strength parameters, pore water pressures, slice weights and external loads. Figure G-12a shows the calculations for the final value of factor of safety (F = 2.23).

*b. Calculation of shear strengths for second-stage computations*. Calculations of the consolidation stresses and undrained shear strengths for the second-stage computations are shown in the table in Figure G-12b. Except for the formula used to compute the total normal force (N) on the bottom of the slices, the calculations are identical to those described in Section G-6b, where the Simplified Bishop Method was used. For the Modified Swedish Method, the total normal force is calculated using Equation G-16.

*c. Second-stage computations*. Except for the procedure used to calculate the factor of safety, the quantities and calculations are the same as those used with the Simplified Bishop Method described in Section G-6c. The second-stage stability calculations in Figure G-13a are for the final value of the factor of safety (F = 1.52).

| 1 | 2 | 3 | 4 | 5 | 6 | 7 | 8 | 9 | 10 | 11 | 12 | 13 | 14 | 15 | 16 | 17 |
|---|---|---|---|---|---|---|---|---|---|---|---|---|---|---|---|---|
| | | | | | Surface loads | | | | | | | | | | | |
| Slice Number | Horizontal Width (b), ft. | Average Slice Height, ft. | Slice Area, sq. ft | Total Weight (W), kips | Height of surface water ($h_s$), ft | Press. At Top of Slice ($P_{surface}$), ksf | Slope at Top of Slice ($\beta$), degs | Length of Top of Slice ($\ell_{top}$), ft | Surface Load (P), kips | Base Inclination ($\alpha$), degs. | Slice Base Length ($\ell$), ft. | Piezometric height ($h_p$), ft. | Pore Water Pressure (u), ksf | Cohesion (c), ksf | Friction Angle ($\phi$), degs. | Interstice Force on Downslope Side ($Z_{i+1}$), kips (Assumed F = 2.23) |
| 1 | 4 | 4 | 14 | 2 | 0 | 0 | 18 | 4 | 0 | 61 | 8 | 0 | 0 | 0 | 30 | 2 |
| 2 | 20 | 21 | 428 | 58 | 0 | 0 | 18 | 20 | 0 | 55 | 35 | 14 | 0.89 | 0 | 30 | 56 |
| 3 | 18 | 45 | 807 | 109 | 0 | 0 | 18 | 18 | 0 | 46 | 26 | 38 | 2.36 | 0 | 30 | 137 |
| 4 | 18 | 58 | 1015 | 137 | 0 | 0 | 18 | 19 | 0 | 40 | 23 | 55 | 3.4 | 0 | 30 | 219 |
| 5 | 28 | 65 | 1785 | 241 | 6 | 0.34 | 18 | 30 | 10 | 32 | 32 | 70 | 4.39 | 0 | 30 | 329 |
| 6 | 22 | 69 | 1508 | 204 | 15 | 0.96 | 18 | 24 | 23 | 24 | 24 | 84 | 5.24 | 0 | 30 | 391 |
| 7 | 23 | 68 | 1570 | 212 | 24 | 1.52 | 18 | 25 | 38 | 18 | 24 | 93 | 5.78 | 0 | 30 | 426 |
| 8 | 22 | 66 | 1449 | 196 | 33 | 2.04 | 18 | 23 | 47 | 11 | 22 | 99 | 6.15 | 0 | 30 | 432 |
| 9 | 31 | 60 | 1844 | 249 | 41 | 2.58 | 18 | 32 | 83 | 4 | 31 | 102 | 6.36 | 0 | 30 | 395 |
| 10 | 35 | 49 | 1702 | 230 | 52 | 3.26 | 18 | 36 | 119 | -5 | 35 | 102 | 6.34 | 0 | 30 | 292 |
| 11 | 30 | 34 | 1005 | 136 | 63 | 3.93 | 18 | 32 | 124 | -14 | 31 | 97 | 6.02 | 0 | 30 | 161 |
| 12 | 33 | 12 | 410 | 55 | 73 | 4.59 | 18 | 35 | 159 | -23 | 35 | 86 | 5.36 | 0 | 30 | 0 |

a. First-stage stability computations

| 1 | 2 | 3 | 4 | 5 | 6 | 7 | 8 | 9 | 10 |
|---|---|---|---|---|---|---|---|---|---|
| Total Normal Force (N), kips | Pore Water Pressure (u), ksf | Effective Normal Stress ($\sigma'_{fc}$), ksf | Shear Force (S), kips | Shear Stress ($\tau_{fc}$), ksf | Consolidation Stress Ratio ($K_c$) | $\tau_{ff}$ ($K_c$ = 1), ksf | $\tau_{ff}$ ($K_c$ = $K_f$), ksf | Effective Prin. Stress ratio at failure, $K_f$ | Interpolated strength ($\tau_{ff}$), ksf |
| 2 | 0 | 0.29 | 1 | 0.08 | 1.70 | 1.47 | 0.17 | 3.00 | 1.01 |
| 74 | 0.89 | 1.24 | 11 | 0.32 | 1.70 | 1.79 | 0.72 | 3.00 | 1.41 |
| 127 | 2.36 | 2.53 | 17 | 0.66 | 1.70 | 2.21 | 1.46 | 3.00 | 1.95 |
| 151 | 3.4 | 3.24 | 19 | 0.84 | 1.70 | 2.44 | 1.87 | 3.00 | 2.24 |
| 262 | 4.39 | 3.69 | 31 | 0.96 | 1.70 | 2.59 | 2.13 | 3.00 | 2.43 |
| 228 | 5.24 | 4.19 | 26 | 1.09 | 1.70 | 2.76 | 2.42 | 3.00 | 2.64 |
| 247 | 5.78 | 4.43 | 28 | 1.15 | 1.70 | 2.83 | 2.56 | 3.00 | 2.74 |
| 239 | 6.15 | 4.51 | 26 | 1.17 | 1.70 | 2.86 | 2.61 | 3.00 | 2.77 |
| 330 | 6.36 | 4.44 | 35 | 1.15 | 1.70 | 2.84 | 2.56 | 3.00 | 2.74 |
| 357 | 6.34 | 3.98 | 36 | 1.03 | 1.70 | 2.69 | 2.3 | 3.00 | 2.55 |
| 281 | 6.02 | 3.09 | 25 | 0.8 | 1.70 | 2.39 | 1.78 | 3.00 | 2.18 |
| 249 | 5.36 | 1.59 | 15 | 0.41 | 1.70 | 1.9 | 0.92 | 3.00 | 1.56 |

b. Strength computations for second stage

Figure G-12. Computations with improved drawdown procedure – Modified Swedish/Spencer's Method – first stage

| 1 | 2 | 3 | 4 | 5 | 6 | 7 | 8 | 9 | 10 | 11 | 12 | 13 | 14 | 15 |
|---|---|---|---|---|---|---|---|---|---|---|---|---|---|---|
| | | | Surface Loads | | | | | | | | | | | |
| Slice Number | Slice Area, sq. ft | Total Weight (W), kips | Height of surface water ($h_s$), ft | Press. At Top of Slice ($P_{surface}$), ksf | Slope at Top of Slice ($\beta$), degs | Length of Top of Slice ($\ell_{top}$), ft | Surface Load (P), kips | Base Inclination ($\alpha$), degs. | Slice Base Length ( $\ell$ ), ft. | Piezometric height ($h_p$), ft. | Pore Water Pressure (u), ksf | Cohesion (c), ksf | Friction Angle ($\phi'$), degs. | Interstice Force on Downslope Side ($Z_{i+1}$), kips (Assumed F = 1.52) |
| 1 | 14 | 2 | 0 | 0 | 18 | 4 | 0 | 61 | 8 | 0 | 0 | 1.01 | 0 | -6 |
| 2 | 428 | 58 | 0 | 0 | 18 | 20 | 0 | 55 | 35 | 0 | 0 | 1.41 | 0 | 14 |
| 3 | 807 | 109 | 0 | 0 | 18 | 18 | 0 | 46 | 26 | 0 | 0 | 1.95 | 0 | 69 |
| 4 | 1015 | 137 | 0 | 0 | 18 | 19 | 0 | 40 | 23 | 0 | 0 | 2.24 | 0 | 130 |
| 5 | 1785 | 241 | 0 | 0 | 18 | 30 | 0 | 32 | 32 | 0 | 0 | 2.43 | 0 | 211 |
| 6 | 1508 | 204 | 0 | 0 | 18 | 24 | 0 | 24 | 24 | 0 | 0 | 2.64 | 0 | 254 |
| 7 | 1570 | 212 | 0 | 0 | 18 | 25 | 0 | 18 | 24 | 0 | 0 | 2.74 | 0 | 275 |
| 8 | 1449 | 196 | 0 | 0 | 18 | 23 | 0 | 11 | 22 | 0 | 0 | 2.77 | 0 | 273 |
| 9 | 1844 | 249 | 0 | 0 | 18 | 32 | 0 | 4 | 31 | 0 | 0 | 2.74 | 0 | 236 |
| 10 | 1702 | 230 | 0 | 0 | 18 | 36 | 0 | -5 | 35 | 0 | 0 | 2.55 | 0 | 156 |
| 11 | 1005 | 136 | 0 | 0 | 18 | 32 | 0 | -14 | 31 | 0 | 0 | 2.18 | 0 | 71 |
| 12 | 410 | 55 | 0 | 0 | 18 | 35 | 0 | -23 | 35 | 0 | 0 | 1.56 | 0 | 0 |

a. Second-stage stability computations

| 1 | 2 | 3 | 4 | 5 | 6 | 7 |
|---|---|---|---|---|---|---|
| Total Normal Force (N), kips | Piezometric height ($h_p$), ft. | "Drained" Pore Pressure (u), ksf | Drained Effective Stress ($\sigma'_{drained}$), ksf | Undrained Shear Strength ($\tau_{ff}$), ksf | Drained Shear Strength ($S_{drained}$), ksf | Lowest Shear Strength - Use for Third Stage |
| -3 | 0 | 0 | -0.41 | 1.01 | 0.00 | Drained |
| 47 | 0 | 0 | 1.35 | 1.41 | 0.78 | Undrained |
| 106 | 0 | 0 | 4.07 | 1.95 | 2.35 | Undrained |
| 133 | 0 | 0 | 5.87 | 2.24 | 3.39 | Undrained |
| 232 | 0 | 0 | 7.13 | 2.43 | 4.12 | Undrained |
| 195 | 5 | 0.31 | 7.75 | 2.64 | 4.47 | Undrained |
| 204 | 14 | 0.85 | 7.59 | 2.74 | 4.38 | Undrained |
| 192 | 20 | 1.22 | 7.33 | 2.77 | 4.23 | Undrained |
| 254 | 23 | 1.43 | 6.86 | 2.74 | 3.96 | Undrained |
| 252 | 23 | 1.41 | 5.88 | 2.55 | 3.40 | Undrained |
| 169 | 18 | 1.09 | 4.38 | 2.18 | 2.53 | Drained |
| 92 | 7 | 0.43 | 2.13 | 1.56 | 1.23 | Drained |

b. Strength computations for third stage

| 1 | 2 | 3 | 4 |
|---|---|---|---|
| Pore Water Pressure (u), ksf | Cohesion (c), ksf | Friction Angle ($\phi'$), degs. | Interstice Force on Downslope Side ($Z_{i+1}$), kips (Assumed F = 1.44) |
| 0 | 0 | 30 | 1 |
| 0 | 0 | 30 | 34 |
| 0 | 1.95 | 0 | 86 |
| 0 | 2.24 | 0 | 144 |
| 0 | 2.43 | 0 | 221 |
| 0 | 2.64 | 0 | 262 |
| 0 | 2.74 | 0 | 281 |
| 0 | 2.77 | 0 | 276 |
| 0 | 2.74 | 0 | 236 |
| 0 | 2.55 | 0 | 152 |
| 0 | 2.18 | 0 | 63 |
| 0.43 | 0 | 30 | 0 |

c. Third-stage stability computations

Figure G-13. Computations with improved drawdown procedure – Modified Swedish/Spencer's Method – second and third stages *d. Evaluation of shear strengths for third-stage computations*. Once the computations for the second stage are completed, drained strengths are computed as shown in Figure G-13b. Except for the equation used to compute the total normal force on the bottom of the slices, the computations are the same as those for the Simplified Bishop Method in Section G-6d.

*e. Third-stage computations*. The quantities for the third-stage computations are summarized in Figure G-13c. As with any analysis using the Modified Swedish Method, a trial value is assumed for the factor of safety, and interslice forces are computed using Equation C-19. The process is repeated with other trial values of factor of safety until the force on the downslope side of the last slice is essentially zero. The interslice force computations in Figure G-13c are shown for the final value of the factor of safety (F = 1.44). This value is the factor of safety after rapid drawdown for this method. This value is the same as the value computed using the Simplified Bishop Method. This is not surprising because the two methods (Spencer and Simplified Bishop) usually give values for the factor of safety that are the same or very nearly the same.

## G-8. Summary of Examples

The results of the three examples discussed above are as follows:

| Example | Method | Factor of Safety |
|---|---|---|
| 1 | Corps of Engineers' (1970) rapid drawdown and stability calculations performed using the Modified Swedish Method, with total side forces inclined at the average slope of the embankment, $\theta$ = 19.4 degrees. | 1.35 |
| 2 | Improved rapid drawdown procedure and stability calculations performed using the Simplified Bishop Method. | 1.44 |
| 3 | Improved rapid drawdown procedure and stability calculations performed using the Modified Swedish Method, with side force inclinations determined using Spencer's Method, $\theta$ = 12.2 degrees for stage 2, and $\theta$ = 13.7 degrees for stage 3. This is the same as Spencer's Method. | 1.44 |

The methods used in Examples 2 and 3 – the improved rapid drawdown procedure, with stability calculations performed using the Simplified Bishop or Spencer's Method – give factors of safety that are slightly higher than the factor of safety computed for example 1. It might seem tempting to conclude that, since the differences in factor of safety shown here are small, the choice between these methods can be made on the basis of which is simpler, or more familiar. However, this would not be a valid conclusion, and should not be used as a justification for continued use of the less accurate Corps of Engineers' (1970) rapid drawdown procedure.

The Corps of Engineers' (1970) rapid drawdown procedure is inherently conservative, because it under-estimates undrained shear strength. Counteracting this conservatism is the fact that the Modified Swedish Method, with total side forces inclined at the average slope of the embankment, overestimates factor of safety as compared with more accurate methods (Simplified Bishop or the Spencer Method). Although these effects nearly balance out for this particular embankment, and the difference in factors of safety is fairly small in this example, there is no reason to believe that this will always be the case. Because the improved procedure for rapid drawdown analysis is based on sound soil mechanics principles and because it employs realistic representations of soil strengths, it provides more meaningful and reliable factors of safety. It should be used, in combination with accurate stability analysis methods (Simplified Bishop or the Spencer Method), on future Corps of Engineers' projects. The minimum required factors of safety to be used with the improved procedure (given in Chapter 3) are 8 to 10 percent higher than those required in the 1970 manual. This consistent with the fact that factors of safety computed using the improved procedure are somewhat higher than those computed using the Corps' drawdown procedure (1970), as noted above.